0022-3565/08/3252-544–555$20.00
THE JOURNAL OF PHARMACOLOGY AND EXPERIMENTAL THERAPEUTICS
JPET 325:544–555, 2008

Vol. 325, No. 2
134783/3329867
Printed in U.S.A.

Noncompetitive Antagonism and Inverse Agonism as Mechanism of Action of Nonpeptidergic Antagonists at Primate and Rodent CXCR3 Chemokine Receptors

Dennis Verzijl, Stefania Storelli, Danny J. Scholten, Leontien Bosch, Todd A. Reinhart, Daniel N. Streblow, Cornelis P. Tensen, Carlos P. Fitzsimons, Guido J. R. Zaman, James E. Pease, Iwan J. P. de Esch, Martine J. Smit, and Rob Leurs

Leiden/Amsterdam Center for Drug Research, Division of Medicinal Chemistry, Vrije Universiteit Amsterdam, Amsterdam, The Netherlands (D.V., S.S., D.J.S., L.B., C.P.F., I.J.P.d.E., M.J.S., R.L.); Department of Infectious Diseases and Microbiology, Graduate School of Public Health, University of Pittsburgh, Pittsburgh, Pennsylvania (T.A.R.); Vaccine and Gene Therapy Institute, Oregon Health and Science University, Beaverton, Oregon (D.N.S.); Department of Dermatology, Leiden University Medical Center, Leiden, The Netherlands (C.P.T.); N.V. Organon, Molecular Pharmacology Unit, Oss, The Netherlands (G.J.R.Z.); and Leukocyte Biology Section, National Heart and Lung Institute, South Kensington Campus, Faculty of Medicine, Imperial College London, London, United Kingdom (J.E.P.)

Received November 28, 2007; accepted February 11, 2008

ABSTRACT

The chemokine receptor CXCR3 is involved in various inflammatory diseases, such as rheumatoid arthritis, multiple sclerosis, psoriasis, and allograft rejection in transplantation patients. The CXCR3 ligands CXCL9, CXCL10, and CXCL11 are expressed at sites of inflammation, and they attract CXCR3-bearing lymphocytes, thus contributing to the inflammatory process. In this study, we characterize five nonpeptidergic compounds of different chemical classes that block the action of CXCL10 and CXCL11 at the human CXCR3, i.e., the 3*H*-pyrido[2,3-*d*]pyrimidin-4-one derivatives *N*-1*R*-[3-(4-ethoxy-phenyl)-4-oxo-3,4-dihydro-pyrido[2,3-*d*]pyrimidin-2-yl]-ethyl-*N*-pyridin-3-ylmethyl-2-(4-fluoro-3-trifluoromethyl-phenyl)-acetamide (VUF10472/NBI-74330) and *N*-1*R*-[3-(4-ethoxy-phenyl)-4-oxo-3,4-dihydro-pyrido[2,3-*d*]pyrimidin-2-yl]-ethyl-*N*-pyridin-3-ylmethyl-2-(4-trifluoromethoxy-phenyl)-acetamide (VUF10085/AMG-487), the 3*H*-quinazolin-4-one decanoic acid {1-[3-(4-cyano-phenyl)-4-oxo-3,4-dihydro-quinazolin-2-yl]-ethyl}-(2-dimethylamino-ethyl)-amide (VUF5834), the imidazolium compound 1,3-bis-[2-(3,4-dichloro-phenyl)-2-oxo-ethyl]-3*H*-imidazol-1-ium bromide (VUF10132), and the quaternary ammonium anilide *N*,*N*-dimethyl-*N*-[4-[[[2-(4-methylphenyl)-6,7-dihydro-5*H*-benzocyclohepten-8-yl]-carbonyl]amino]benzyl] tetrahydro-2*H*-pyran-4-aminium chloride (TAK-779). To understand the action of these CXCR3 antagonists in various animal models of disease, the compounds were also tested at rat and mouse CXCR3, as well as at CXCR3 from rhesus macaque, which was cloned and characterized for the first time in this study. Except for TAK-779, all compounds show slightly lower affinity for rodent CXCR3 than for primate CXCR3. In addition, we have characterized the molecular mechanism of action of the various antagonists at the human CXCR3 receptor. All tested compounds act as noncompetitive antagonists at CXCR3. Moreover, this noncompetitive behavior is accompanied by inverse agonistic properties of all five compounds as determined on an identified constitutively active mutant of CXCR3, CXCR3 N3.35A. It is interesting to note that all compounds except TAK-779 act as full inverse agonists at CXCR3 N3.35A. TAK-779 shows weak partial inverse agonism at CXCR3 N3.35A, and it probably has a different mode of interaction with CXCR3 than the other two classes of small-molecule inverse agonists.

This work was supported in part by grants from The Nederlandse Organistatie voor Wetenschappe-lijk Onderzoek (NWO; to M.J.S.). S.S. was supported by an NWO-Stichting Technische Wetenschappen Pioneer grant (to R.L.), Dutch Top Institute Pharma (to D.J.S. and L.B.), Dutch Cancer Society Grant RUL 2000-2168 (to C.P.T.), and the National Institutes of Health Grant AI060422 (to T.A.R.).

S.S. and D.J.S. contributed equally to this work.

Article, publication date, and citation information can be found at http://jpet.aspetjournals.org.
doi:10.1124/jpet.107.134783.

Chemokines are secreted peptides that are important mediators in inflammation. They are classified into four families based on the number and position of conserved N-terminal cysteine residues, i.e., CC, CXC, CX_3C, and XC chemokines (Murphy et al., 2000). Chemokines bind to a subset of G protein-coupled receptors (GPCRs) of class A, which are named based on their specific chemokine preferences (Mur-

ABBREVIATIONS: GPCR, G protein-coupled receptor; CAM, constitutively active mutant; FBS, fetal bovine serum; PCR, polymerase chain reaction; HEK, human embryonic kidney; ELISA, enzyme-linked immunosorbent assay; PBS, phosphate-buffered saline; BSA, bovine serum albumin; InsP, inositol phosphates; TBS, Tris-buffered saline; PLC, phospholipase C; TM, transmembrane; WT, wild type; H_xR, histamine H_x receptor.

phy et al., 2000). The chemokine receptor CXCR3 is mainly expressed on activated T-helper 1 cells, but also on B cells and natural killer cells (Qin et al., 1998). CXCR3 is activated by the interferon-γ-inducible chemokines CXCL9, CXCL10, and CXCL11, with CXCL11 having the highest affinity (Loetscher et al., 1996; Cole et al., 1998). Upon activation, CXCR3 activates pertussis toxin-sensitive G proteins of the $G\alpha_i$ class and it mediates, e.g., chemotaxis, calcium flux, and activation of kinases such as p44/p42 mitogen-activated protein kinase and Akt (Smit et al., 2003).

CXCR3 and its ligands are up-regulated in a variety of inflammatory diseases, implying a role for CXCR3 in, e.g., rheumatoid arthritis (Qin et al., 1998), multiple sclerosis (Sørensen et al., 1999), transplant rejection (Hancock et al., 2000), atherosclerosis (Mach et al., 1999), and inflammatory skin diseases (Flier et al., 2001). The role of CXCR3 in cancer is two-fold: CXCR3 may be involved in the metastasis of CXCR3-expressing cancer cells (Walser et al., 2006), whereas expression of CXCL10 (Luster and Leder, 1993) or CXCL11 (Hensbergen et al., 2005) at tumor sites may attract CXCR3-expressing immune cells that help control tumor growth and metastasis.

Several animal models have been developed for CXCR3, among which a murine model of metastatic breast cancer (Walser et al., 2006), a murine model of renal cell carcinoma (Pan et al., 2006), and an arthritis model in Lewis rats (Salomon et al., 2002). In a mouse rheumatoid arthritis model, TAK-779, a small-molecule antagonist with affinity for CCR5, CCR2b, and CXCR3, inhibits the development of arthritis by down-regulating T-cell migration, indicating that targeting chemokine receptors in models of inflammation is feasible and effective (Baba et al., 1999; Yang et al., 2002; Gao et al., 2003).

Several classes of small-molecule compounds targeting CXCR3 have recently been described, including 4-*N*-aryl-[1,4]diazepane ureas (Cole et al., 2006), 1-aryl-3-piperidin-4-yl-urea derivatives (Allen et al., 2007), quinazolin-4-one, 3*H*-pyrido[2,3-*d*]pyrimidin-4-one derivatives (Heise et al., 2005; Storelli et al., 2005; Johnson et al., 2007; Storelli et al., 2007), and the above-mentioned quaternary ammonium anilide TAK-779 (Gao et al., 2003). So far, no detailed information is available on the molecular mechanism of action of these small-molecule antagonists at the CXCR3 receptor, despite the general notion that small molecule ligands probably will not have overlapping binding sites with the chemokines, which are supposed to bind mainly to the N terminus and extracellular receptor loops (Murphy et al., 2000). Moreover, although most compounds have been tested on human CXCR3 using in vitro assays, little or no information on their affinity for CXCR3 of other species is available. Especially in view of rodent models of inflammatory diseases it is important to know the relative affinities of the compounds for the receptors of different species.

In this study, we report on the molecular characterization of the 3*H*-pyrido[2,3-*d*]pyrimidin-4-one derivatives VUF10472 (NBI-74330) (Heise et al., 2005; Storelli et al., 2007) and VUF10085 (AMG-487) (Johnson et al., 2007; Storelli et al., 2007); the 3*H*-quinazolin-4-one VUF5834 (Storelli et al., 2005; Johnson et al., 2007); the imidazolium compound VUF10132 (Axten et al., 2003); and the quaternary ammonium anilide TAK-779 (Baba et al., 1999) at CXCR3 of human (Loetscher et al., 1996), rat (Wang et al., 2000), and mouse (Tamaru et al., 1998; Lu et al., 1999). In addition, CXCR3 from rhesus macaque was cloned, characterized, and subjected to a detailed pharmacological analysis using the nonpeptidergic compounds. Moreover, we constructed and characterized a constitutively active mutant (CAM) of CXCR3, which was used to further determine the inverse agonistic properties of the small-molecule compounds.

Materials and Methods

Materials. Dulbecco's modified Eagle's medium and trypsin were purchased from PAA Laboratories GmbH (Paschen, Austria), RPMI 1640 medium with GlutaMAX-I and 25 mM HEPES, nonessential amino acids, sodium pyruvate, and 2-mercaptoethanol were from Sigma-Aldrich (St. Louis, MO), penicillin and streptomycin were obtained from Lonza (Verviers, Belgium), fetal bovine serum (FBS) was purchased from Integro B.V. (Dieren, The Netherlands), and certified FBS was from Invitrogen (Paisley, UK). *myo*-[2-^{3}H]Inositol (10–20 Ci/mmol) was purchased from GE Healthcare (Chalfont St. Giles, UK). ^{125}I-CXCL10 (2200 Ci/mmol) and ^{125}I-CXCL11 (2000 Ci/mmol) were obtained from PerkinElmer Life and Analytical Sciences (Boston, MA). Chemokines were obtained from PeproTech (Rocky Hill, NJ). TAK-779 was obtained from the National Institutes of Health AIDS research and reference reagent program.

DNA Constructs. The cDNA of human CXCR3 inserted in pcDNA3 (Loetscher et al., 1996) was amplified by PCR and inserted into pcDEF3 (a gift from Dr. Langer, Robert Wood Johnson Medical School, Piscataway, NJ).

A cDNA containing the rhesus macaque (*Macaca mulatta*; GenBank accession no. EU313340) CXCR3 open reading frame was obtained from rhesus macaque peripheral blood mononuclear cells that were stimulated overnight with phytohemagglutinin-P plus phorbol myristate acetate. Total RNA was extracted using TRIzol (Invitrogen), and cDNA was generated by reverse transcription with avian myeloblastosis virus reverse transcriptase (Promega, Madison, WI) and oligo(dT) primer. PCR was then performed with Taq polymerase (Promega) and primers TRCXCR3F2 (5′-AGCCCAGCCATGGTCCTTG-3′) and TRCXCR3R2 (5′-CCTCACAAGCCCGAGTAGGA-3′). The resulting PCR product was spin-column purified (QIAGEN GmbH, Hilden, Germany), and it was ligated to pGEM-T vector (Promega). Later, the cDNA was subcloned into pcDEF3.

A cDNA containing the *Rattus norvegicus* CXCR3 open reading frame was cloned from an F344 heart allograft that was transplanted into a Lewis rat at 28 days after transplantation (Streblow et al., 2003). Total RNA was prepared from 0.25 g of rat tissue using the TRIzol method. First-strand cDNA was synthesized from 2 μg of total RNA using 1.0 μM oligo(dT)-T7 primer [GGCCAGTGAATTGTAATACGACTCACTATAGGG$(A)_{24}$] and 200 U of SuperScript III reverse transcriptase (Invitrogen). Doubled-stranded cDNA was generated by the addition of second-strand buffer (Invitrogen) according to the manufacturer's protocol, and it was purified by phenol/chloroform extraction. PCR was performed with Taq DNA polymerase and primers ratCXCR3Fwd: ATAGGATTCATGTACCTTGAGGTCAGTGAACGTCA and ratCXCR3Rev: ATAGAATTCTTACAAGCCCAAGTAGGAGGCCTCAGT. The resulting PCR fragment was cloned into pGEM-Teasy (Promega), and it was subcloned into pcDEF3.

The cDNA of mouse CXCR3 was a kind gift from Dr. Luster (Harvard Medical School, Charlestown, MA) (Lu et al., 1999), and it was subcloned into pcDEF3. The chimeric G protein $G\alpha_{qi5}$ (pcDNA1-HA-m$G\alpha_{qi5}$) was a gift from Dr. Conklin (University of California at San Francisco, San Francisco, CA) (Coward et al., 1999). Other plasmids that were used were pcDNA3.1-CXCR1, pcDEF3-CXCR2, pcDNA3-CXCR4, pcDEF3-CCR1, pcDNA3.1-CCR2, pcDEF3-H_1, and pCIneo-H_3(445).

Synthesis of Small-Molecule Compounds. Synthesis of VUF5834 (Storelli et al., 2005), VUF10472, and VUF10085 (Storelli et al., 2007) has been described previously.

Synthesis of VUF10132 was adapted from the procedure described

by Axten et al. (2003). In brief, 1-(3,4-dichloro-phenyl)-2-imidazol-1-yl-ethanone (0.19 g; 0.75 mmol) and 2-bromo-1-(3,4-dichloro-phenyl)-ethanone (0.20 g; 0.75 mmol) were stirred in acetonitrile (50 ml) overnight at room temperature. The mixture was diluted with ether, and the solid product was filtered, washed with ether, and dried to afford VUF10132 as white solid. Yield: 0.31 g (78%). ^{1}H NMR (dimethyl sulfoxide) δ: 6.20 (s, 4H), 7.67 to 7.80 (m, 4H), 7.88 to 8.12 (m, 3H), 8.23 to 8.25 (m, 2H), 9.12 (s, 1H).

Cell Culture and Transfection. HEK293T cells were grown at 5% CO_2 at 37°C in Dulbecco's modified Eagle's medium supplemented with 10% fetal bovine serum, penicillin, and streptomycin. HEK293T cells were transfected with 2.5 μg of cDNA encoding CXCR3 supplemented with 2.5 μg of pcDNA1-HA-mGα_{qi5} [for phospholipase C (PLC) activation experiments and ELISA] or 2.5 μg of pcDEF3 by using linear polyethyleneimine (mol. wt. 25,000; Polysciences, Warrington, PA). The total amount of DNA in gene-dosing experiments was kept constant at 5 μg by addition of pcDEF3. In brief, 5 μg of DNA in total was diluted in 250 μl of 150 mM NaCl. Later, 30 μg of polyethyleneimine in 250 μl of 150 mM NaCl was added to the DNA solution, and then the solution was incubated for 10 min at room temperature. The mixture was added to adherent HEK293T cells in 100 mM tissue culture dishes. The next day, cells were trypsinized, resuspended into culture medium, and plated in the appropriate poly-L-lysine (Sigma-Aldrich)-coated assay plates. For membrane preparation, cells were harvested 48 h after transfection from the tissue culture dishes in which they were transfected.

Murine pre-B L1.2 cells were grown in RPMI 1640 medium with GlutaMAX-I and 25 mM HEPES, supplemented with 10% heat-inactivated certified FBS, penicillin, streptomycin, glutamine, non-essential amino acids, 2-mercaptoethanol, and sodium pyruvate. L1.2 cells were transfected with 10 μg/20 million cells using a Bio-Rad Gene Pulser II (330 V and 975 μF; Bio-Rad, Hemel Hempstead, UK), and they were grown in culture medium supplemented with 10 mM sodium butyrate.

Chemokine Binding. Cell membrane fractions from transiently transfected HEK293T (CXCR3 and CXCR4) or COS-7 (CXCR2) cells were prepared as follows. Cells were washed with ice-cold PBS, detached using ice-cold PBS containing 1 mm EDTA, and centrifuged at 1500*g* for 10 min at 4°C. Later, cells were washed with PBS and centrifuged at 1500*g* for 10 min at 4°C. The pellet was resuspended in ice-cold membrane buffer (15 mM Tris, pH 7.5, 1 mM EGTA, 0.3 mM EDTA, and 2 mM $MgCl_2$), and then it was homogenized by 10 strokes at 1100 to 1200 rpm using a Teflon-glass homogenizer and rotor. The membranes were subjected to two freeze-thaw cycles using liquid nitrogen, and they were centrifuged at 40,000*g* for 25 min at 4°C. The pellet was rinsed with ice-cold Tris-sucrose buffer (20 mM Tris, pH 7.4, and 250 mM sucrose), and then it was resuspended in the same buffer and frozen in liquid nitrogen. Protein concentration was determined using a Bio-Rad protein assay. Membranes were incubated in 96-well plates in binding buffer (50 mM HEPES, pH 7.4, 1 mM $CaCl_2$, 5 mM $MgCl_2$, 100 mM NaCl, and 0.5% BSA for CXCR3 and CXCR4 radioligand binding assays and 50 mM Na_2/K-phosphate buffer, pH 7.4, and 0.5% BSA for CXCR2 radioligand binding assay) with approximately 50 pM ^{125}I-chemokine and displacer for 2 h at room temperature. Later, membranes were harvested via filtration through Unifilter GF/C plates (PerkinElmer Life and Analytical Sciences) that were pretreated with 1% polyethylenimine, and then they were washed three times with ice-cold wash buffer (50 mM HEPES, pH 7.4, 1 mM $CaCl_2$, 5 mM $MgCl_2$, and 500 mM NaCl for CXCR3 and CXCR4 and 50 mM Na_2/K-phosphate buffer, pH 7.4, for CXCR2). Radioactivity was measured using a MicroBeta (PerkinElmer Life and Analytical Sciences).

Histamine H_1 Receptor Binding. Cell homogenates from COS-7 cells transiently transfected with cDNA encoding the human histamine H_1 receptor were incubated with 7 nM [^{3}H]mepyramine and 10 μM CXCR3 antagonist in H_1 buffer (50 mM Na_2/K-phosphate buffer, pH 7.4) for 30 min at room temperature, and then they were harvested via filtration using ice-cold H_1 buffer as described above.

Phospholipase C Activation. Twenty-four hours after transfection, HEK293T cells were labeled overnight in Earle's inositol-free minimal essential medium (Invitrogen) supplemented with 10% fetal bovine serum, penicillin, and streptomycin and with *myo*-[2-^{3}H]-inositol (1 μCi/ml). Cells were washed with inositol phosphates (InsP) assay buffer [20 mM HEPES, pH 7.4, 140 mM NaCl, 5 mM KCl, 1 mM $MgSO_4$, 1 mM $CaCl_2$, 10 mM glucose, and 0.05% (w/v) BSA], and then they were incubated for 2 h in InsP assay buffer supplemented with 10 mM LiCl in the presence or absence of indicated ligands. The incubation was stopped by aspiration of the assay buffer and addition of ice-cold 10 mM formic acid. After incubation for 90 min at 4°C, [^{3}H]InsP were isolated by anion exchange chromatography (Dowex AG1-X8 columns; Bio-Rad) and counted by liquid scintillation.

Chemotaxis. Twenty-four hours after transfection, chemotaxis of L1.2 cells toward 10 nM CXCL10 was determined in the presence or absence of small-molecule compounds, using 5-μm pore ChemoTx 96-well plates (Neuro Probe, Inc., Gaithersburg, MD). In brief, ChemoTx plates were blocked using RPMI 1640 medium with GlutaMAX-I and 25 mM HEPES supplemented with 1% (w/v) BSA. Chemokine and compound dilutions were made in RPMI 1640 medium with GlutaMAX-I and 25 mM HEPES supplemented with 0.1% (w/v) BSA, and samples were added to the wells. L1.2 cells were added on top of the membrane and incubated for 5 h in a humidified chamber at 37°C. The number of migrated cells per well was determined using a hemocytometer.

Enzyme-Linked Immunosorbent Assay. Forty-eight hours after transfection, HEK293T cells were washed with TBS, and then they were fixed with 4% paraformaldehyde in PBS. After blocking with 1% skim milk in 0.1 M $NaHCO_3$, pH 8.6, cells were incubated with mouse monoclonal anti-CXCR3 antibody (MAB160; R&D Systems, Minneapolis, MN) in TBS containing 0.1% BSA, washed three times with TBS, and then incubated with goat anti-mouse horseradish peroxidase-conjugated secondary antibody (Bio-Rad). Later, cells were incubated with substrate buffer containing 2 mM *o*-phenylenediamine (Sigma-Aldrich), 35 mM citric acid, 66 mM Na_2HPO_4, and 0.015% H_2O_2, pH 5.6. The reaction was stopped with 1 M H_2SO_4, and absorption at 490 nm was determined.

Data Analysis. Nonlinear regression analysis of the data and calculation of K_d and K_i values was performed using Prism 4.03 (GraphPad Software Inc., San Diego, CA). The pK_b values in the PLC activation assay were calculated using the Cheng-Prusoff equation $pK_b = IC_{50}/(1 + [\text{agonist}]/EC_{50})$ (Cheng and Prusoff, 1973).

Results

Nonpeptidergic CXCR3 Antagonists. A selection of CXCR3-targeting small-molecule antagonists from two different structural classes were synthesized as described previously, and then they were subjected to detailed pharmacological analysis: quinazolinone-derived 3*H*-pyrido[2,3-*d*]pyrimidin-4-one compounds VUF10472 (NBI-74330) (Heise et al., 2005; Storelli et al., 2007) and VUF10085 (AMG 487) (Johnson et al., 2007; Storelli et al., 2007), the 3*H*-quinazolin-4-one VUF5834 (Storelli et al., 2005; Johnson et al., 2007), and the imidazolium compound VUF10132 (Axten et al., 2003) (Fig. 1). The well described CCR5 antagonist TAK-779 (Baba et al., 1999) has been reported to show affinity for mouse CXCR3 (Gao et al., 2003); therefore, it was included in our set of small-molecule compounds as well (Fig. 1).

Characterization of Human CXCR3. Binding studies were performed with radiolabeled CXCL10 and CXCL11 on membranes prepared from HEK293T cells transiently transfected with cDNA encoding human CXCR3 (Loetscher et al., 1996). Homologous displacement of the radioligands with unlabeled chemokines resulted in pK_d values ± S.E.M. of

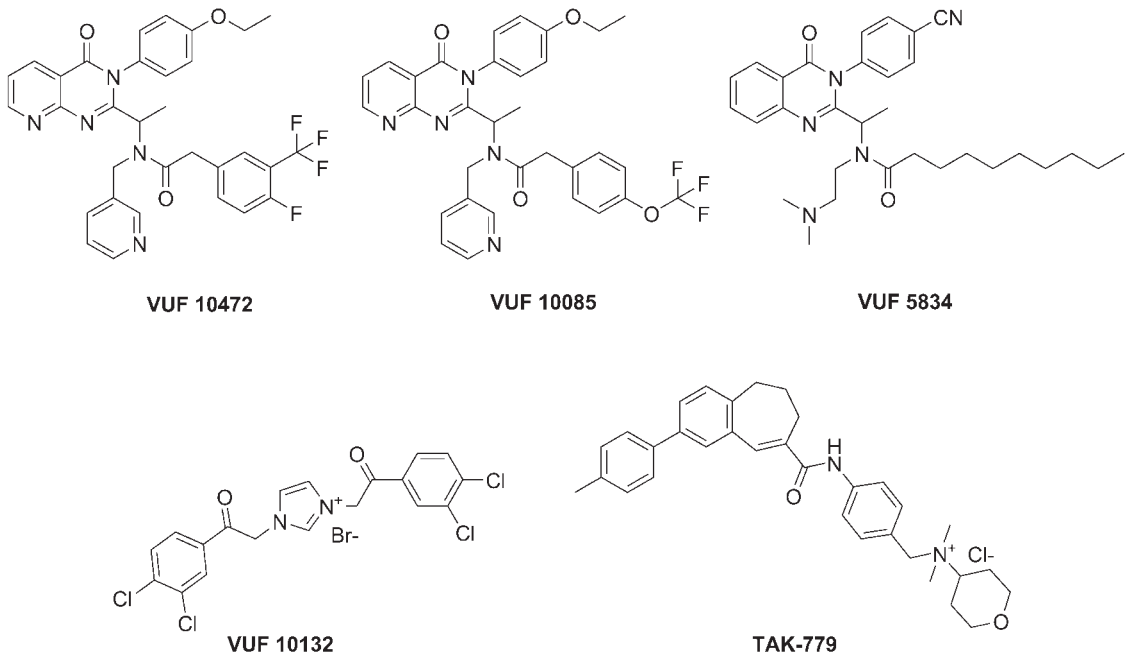

Fig. 1. Structures of small-nonpeptidergic compounds targeting CXCR3. The structures of NBI-74330; *N*-1*R*-[3-(4-ethoxy-phenyl)-4-oxo-3,4-dihydro-pyrido[2,3-*d*]pyrimidin-2-yl]-ethyl-*N*-pyridin-3-ylmethyl-2-(4-fluoro-3-trifluoromethyl-phenyl)-acetamide (VUF10472), AMG-487; *N*-1*R*-[3-(4-ethoxy-phenyl)-4-oxo-3,4-dihydro-pyrido[2,3-*d*]pyrimidin-2-yl]-ethyl-*N*-pyridin-3-ylmethyl-2-(4-trifluoromethoxy-phenyl)-acetamide (VUF10472), decanoic acid {1-[3-(4-cyano-phenyl)-4-oxo-3,4-dihydro-quinazolin-2-yl]-ethyl}-(2-dimethylamino-ethyl)-amide (VUF5834), 1,3-bis-[2-(3,4-dichloro-phenyl)-2-oxo-ethyl]-3*H*-imidazol-1-ium bromide (VUF10132), and *N*,*N*-dimethyl-*N*-[4-[[[2-(4-methylphenyl)-6,7-dihydro-5*H*-benzocyclohepten-8-yl]carbonyl]amino]benzyl] tetrahydro-2*H*-pyran-4-aminium chloride (TAK-779) are shown.

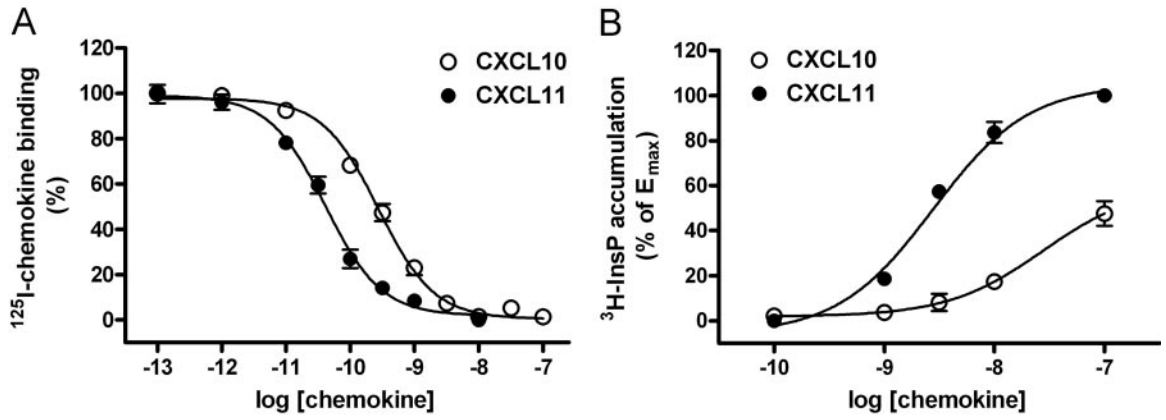

Fig. 2. Characterization of human CXCR3. A, homologous displacement binding at human CXCR3. Binding experiments were performed with approximately 50 pM ^{125}I-CXCL10 (○) or ^{125}I-CXCL11 (●) and increasing concentrations of homologous unlabeled chemokine on membranes from HEK293T cells transfected with cDNA encoding human CXCR3. Data are presented as percentage of total binding. pK_d values for CXCL10 and CXCL11 were 9.8 ± 0.1 (n = 11) and 10.6 ± 0.1 (n = 7), respectively. B, activation of PLC by human CXCR3. HEK293T cells were transfected with cDNA encoding human CXCR3 and Gα_{qi5}. After 48 h, [^{3}H]InsP accumulation was determined in the presence of increasing concentrations of CXCL10 (○) or CXCL11 (●). Data are presented as a percentage of the maximal response obtained with 100 nM CXCL11. pEC_{50} values for CXCL10 and CXCL11 were 7.5 ± 0.1 (n = 8) and 8.5 ± 0.1 (n = 12), respectively.

TABLE 1

Properties of chemokine ligands at CXCR3

The pK_d values and B_{max} values ± S.E.M. are shown for human CXCL10 and human CXCL11 at the various CXCR3, calculated from homologous radioligand binding experiments. pEC_{50} values ± S.E.M. were obtained using the PLC activation assay.

Species	Human CXCL10						Human CXCL11					
	pK_d	n	B_{max}	n	pEC_{50}	n	pK_d	n	B_{max}	n	pEC_{50}	n
Human	9.8 ± 0.1	11	358 ± 53	6	7.5 ± 0.1	8	10.6 ± 0.1	7	407 ± 126	4	8.5 ± 0.1	12
N3.35A	10.2 ± 0.2	4	327 ± 91	4	7.5 ± 0.0	2	11.3 ± 0.3	3	564 ± 242	3	8.7 ± 0.1	4
Rhesus	10.0 ± 0.1	3	163 ± 7	2	7.4 ± 0.1	3	10.8 ± 0.3	3	255 ± 114	4	8.5 ± 0.1	3
Rat	10.2 ± 0.2	7	631 ± 141	7	8.8 ± 0.1	3	10.7 ± 0.2	4	1170 ± 644	3	9.5 ± 0.1	3
Mouse	10.1 ± 0.1	3	658 ± 127	3	8.3 ± 0.1	5	10.7 ± 0.3	4	1882 ± 858	4	9.2 ± 0.2	3

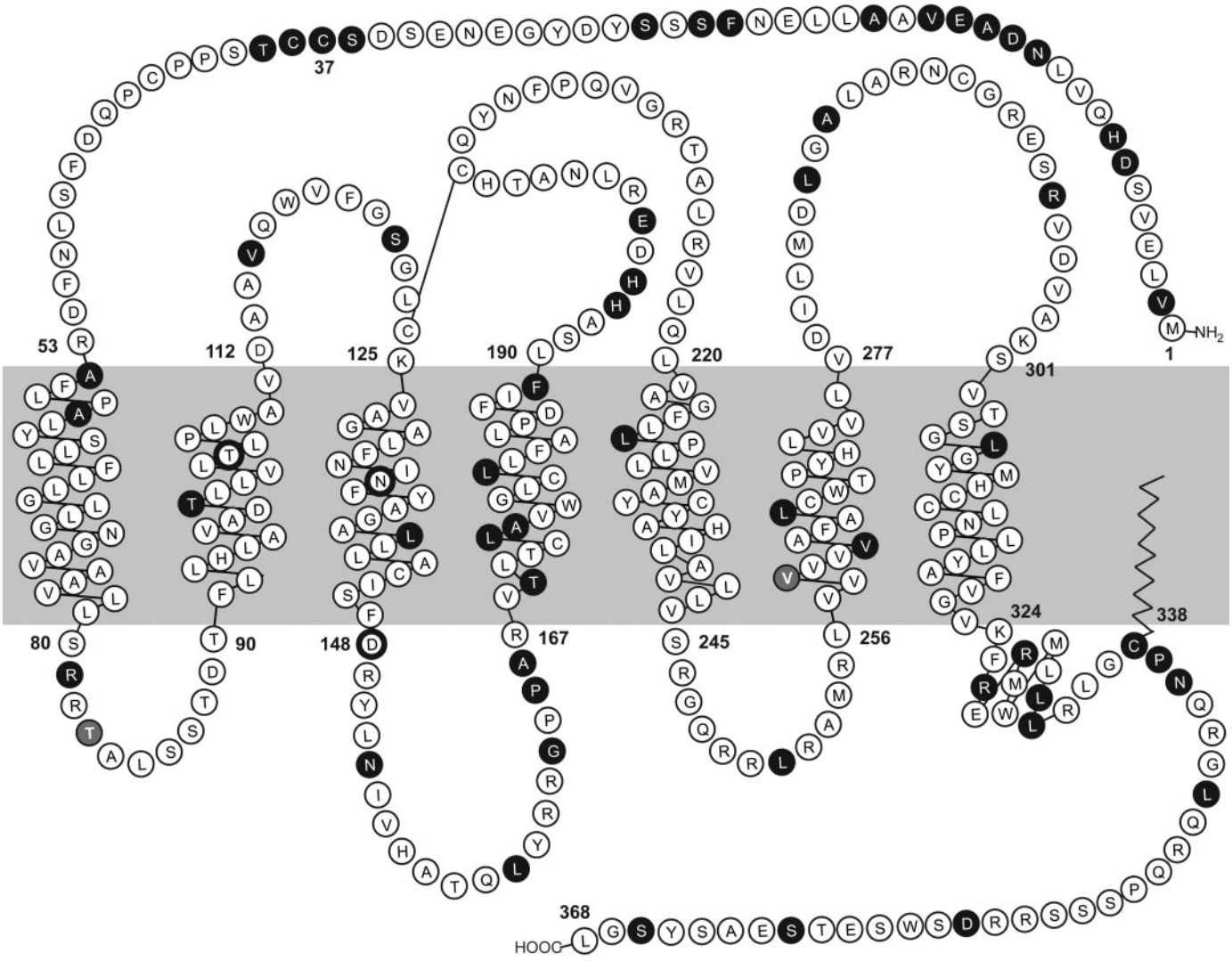

Fig. 3. Snakeplot of CXCR3. Amino acids that were mutated to generate constitutively active mutants (T2.56, N3.35, and D3.49) are indicated as bold circled residues. Amino acids that differ between human and rhesus macaque CXCR3 (T^{83} in intracellular loop 1 and V6.39 are both Ala in rhesus macaque CXCR3) are shown as gray circles. Residues that are different between primate and rodent (i.e., rat and/or mouse) CXCR3 are indicated as black circles. Human and rhesus macaque CXCR3 have an additional Cys (C^{37}) in their amino terminus compared with rat and mouse CXCR3. Helix 8 at the membrane-proximal part of the carboxyl terminus and potential palmitoylation of Cys^{338} are shown as well.

9.8 ± 0.1 for CXCL10 and 10.6 ± 0.1 for CXCL11 (Fig. 2A; Table 1), in accordance with the values and rank order for these chemokines reported in literature (Cole et al., 1998; Heise et al., 2005).

In HEK293 cells, human CXCR3 does not couple efficiently to the PLC-InsP pathway (Wang et al., 2000). Therefore, CXCR3 was transiently cotransfected with cDNA encoding the chimeric G protein $G\alpha_{qi5}$ (Coward et al., 1999), after which robust PLC activation could be observed upon stimulation with CXCL10 and CXCL11. Using this functional assay, pEC_{50} values of 7.5 ± 0.1 and 8.5 ± 0.1 were obtained for CXCL10 and CXCL11, respectively (Fig. 2B; Table 1). CXCL10 acted as a partial agonist, with an intrinsic activity of 0.48 ± 0.8 compared with the full agonist CXCL11 (Fig. 2B; $n = 5$).

Characterization of Rhesus Macaque, Rat, and Mouse CXCR3. Because the affinities of small-molecule compounds targeting chemokine receptors may differ among species, e.g., for TAK-779 at human and mouse CCR5 (Baba et al., 1999; Gao et al., 2003), and significant differences between the amino acid sequences of human and rodent CXCR3 are apparent (Fig. 3), we set out to characterize CXCR3 of rhesus macaque, mouse, and rat. CXCR3 of mouse (Tamaru et al., 1998; Lu et al., 1999) and rat (Wang et al., 2000) have been cloned and described previously. Here, we report the cloning and characterization of rhesus macaque CXCR3 from peripheral blood mononuclear cells (GenBank accession no. EU313340; see *Materials and Methods*). The deduced amino acid sequence of rhesus macaque CXCR3 was found to be 99% identical to human CXCR3. The Thr^{83} residue in the first intracellular loop of human CXCR3 is Ala^{83} in rhesus macaque CXCR3, and Val^{259} at position 6.39[1] in TM6 of human CXCR3 is Ala^{259} in rhesus macaque CXCR3 (Fig. 3).

After expression in HEK293T cells, CXCR3 from rhesus,

[1] GPCR numbering according to Ballesteros and Weinstein (1995), where the first digit refers to the transmembrane helix, and the second number indicates the position of the residue relative to the most conserved amino acid, which is assigned position 50 in that helix (i.e., N1.50, D2.50, R3.50, W4.50, P5.50, P6.50, and P7.50).

rat, and mouse showed similar binding affinities for human CXCL10 and CXCL11 as human CXCR3 (Table 1). B_{max} values of rodent CXCR3 were increased compared with human CXCR3, approximately 2-fold higher for CXCL10 and 3- to 4-fold higher for CXCL11 (Table 1) when equal amounts of cDNA were transfected. The B_{max} value for CXCL10 at rhesus CXCR3 was 2-fold lower than for human CXCR3, whereas human and rhesus CXCR3 had comparable B_{max} values for CXCL11 (Table 1). Rhesus CXCR3 stimulated PLC with similar maximal effect (E_{max}) and similar EC_{50} values for human CXCL10 and CXCL11 as human CXCR3 (Fig. 4, A and B; Table 1). In contrast, the rodent CXCR3 species had approximately 10-fold higher potencies and showed increased E_{max} for human CXCL10 compared with human CXCR3 (Fig. 4, A and B; Table 1). The E_{max} for human CXCL11 at rat CXCR3 was also increased compared with the effect of CXCL11 at CXCR3 of the other species (Fig. 4B).

Behavior of Nonpeptidergic Compounds at CXCR3. The panel of small-molecule antagonists inhibited ^{125}I-CXCL10 binding to human CXCR3, with K_i values ranging between 4 nM for VUF10472 and 1.3 μM for TAK-779 (Fig. 5A; Table 2). VUF10085, VUF5834, and VUF10132 showed intermediate K_i values of 20, 158, and 251 nM, respectively (Fig. 5A; Table 2). Subsequently, the ability of the small molecules to inhibit CXCL10-induced PLC activation through human CXCR3 was determined. All compounds reduced CXCL10-mediated (10–50 nM) PLC activation, with K_b values ranging from 6 nM for VUF10472 to 800 nM for TAK-779 (Fig. 5B; Table 2). A good correlation ($r^2 = 0.997$) was observed between the measured pK_i values and pK_b values determined against CXCL10 (Fig. 5C). For the most potent compound, VUF10472, inhibition of CXCL11-induced (5 nM) PLC activation was also determined, resulting in a K_b value of 12.6 nM (Fig. 5D). This value corresponds well to the value obtained against CXCL10 (Fig. 5D; Table 2). Finally, the ability of the small-molecule compounds to inhibit chemotaxis was investigated. The murine pre-B cell line L1.2 was transiently transfected with cDNA encoding human CXCR3, and migration of cells toward CXCL10 in the presence or absence of VUF10085 and VUF5834 was determined. CXCR3-transfected L1.2 cells did not migrate in the absence of CXCL10, whereas 10.3 ± 0.8% ($n = 3$) of the cells migrated to 10 nM CXCL10 in the absence of inhibitors (Fig. 5E, inset). Both compounds completely inhibited 10 nM CXCL10-induced migration at a concentration of 10 μM, with pIC_{50} values of 6.8 ± 0.2 ($n = 2$) and 5.8 ± 0.1 ($n = 3$) for VUF10085 and VUF5834, respectively (Fig. 5E).

Next, the affinity of the small-molecule compounds for CXCR3 of the different species was determined using ^{125}I-CXCL10. The pK_i values of the compounds tested at rhesus CXCR3 were identical to the values found for human CXCR3 (Table 2). Likewise, the affinities of the compounds tested at rat and mouse CXCR3 were identical to each other. However, VUF10472, VUF10085, VUF5834, and VUF10132 showed an approximately 4-fold lower affinity for the rodent CXCR3 (mouse and rat) compared with the primate CXCR3 (human and rhesus). Only for TAK-779 no difference in affinity between CXCR3 from the different species was observed.

Because the nonpeptidergic compounds showed slightly lower affinity for rodent CXCR3 and the previous experiments were performed with human chemokines, we also determined the ability of the antagonists to inhibit mouse CXCL10-induced signaling at mouse CXCR3. The pEC_{50} of mouse CXCL10 at mouse CXCR3 (8.4 ± 0.1; $n = 3$) was comparable with the pEC_{50} of human CXCL10 at mouse CXCR3 (8.3 ± 0.1; $n = 5$). The different antagonists inhibited mouse CXCL10-induced activation of mouse CXCR3 (measured as PLC stimulation), with K_b values ranging from 4 nM for VUF10472 to 400 nM for TAK-779. The K_b values obtained under these conditions are within 2-fold of the K_b values for inhibition of human CXCL10 at human CXCR3 (Fig. 5F; Table 2).

To determine whether the antagonists show competitive or noncompetitive behavior, a Schild analysis was performed. HEK293T cells expressing human CXCR3 and $G\alpha_{qi5}$ were incubated with increasing concentrations of CXCL10 (Fig. 6A) or CXCL11 (Fig. 6B) in the absence or presence of different concentrations of VUF10472. A decreased maximal effect combined with a rightward shift of the curves was observed in the presence of VUF10472, indicating noncompetitive antagonist behavior. The mechanism of antagonism of the other classes of small-molecule compounds was investigated using

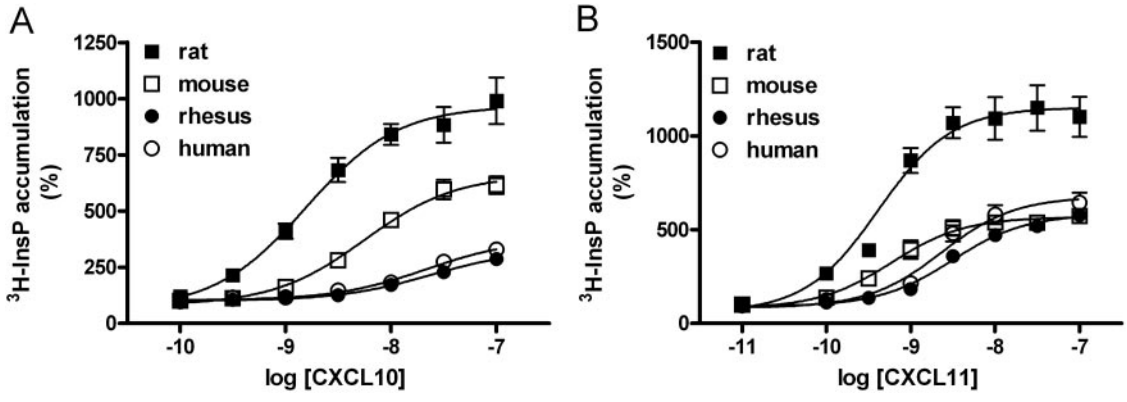

Fig. 4. Activation of PLC by primate and rodent CXCR3. A, CXCL10-induced activation of PLC. HEK293T cells were transfected with cDNA encoding human, rhesus, rat, or mouse CXCR3 and $G\alpha_{qi5}$. After 48 h, [^{3}H]InsP accumulation was determined in the presence of increasing concentrations of human CXCL10. pEC_{50} values for CXCL10 were 7.5 ± 0.1 (human CXCR3; $n = 8$), 7.4 ± 0.1 (rhesus CXCR3; $n = 3$), 8.8 ± 0.1 (rat CXCR3; $n = 3$), and 8.3 ± 0.1 (mouse CXCR3; $n = 5$). B, CXCL11-induced activation of PLC. HEK293T cells were transfected with cDNA encoding human, rhesus, rat, or mouse CXCR3 and $G\alpha_{qi5}$. After 48 h, [^{3}H]InsP accumulation was determined in the presence of increasing concentrations of human CXCL11. pEC_{50} values for CXCL11 were 8.5 ± 0.1 (human CXCR3; $n = 12$), 8.5 ± 0.1 (rhesus CXCR3; $n = 3$), 9.5 ± 0.1 (rat CXCR3; $n = 3$), and 9.2 ± 0.2 (mouse CXCR3; $n = 3$). Data are presented per receptor as a percentage of [^{3}H]InsP accumulation in the absence of chemokine.

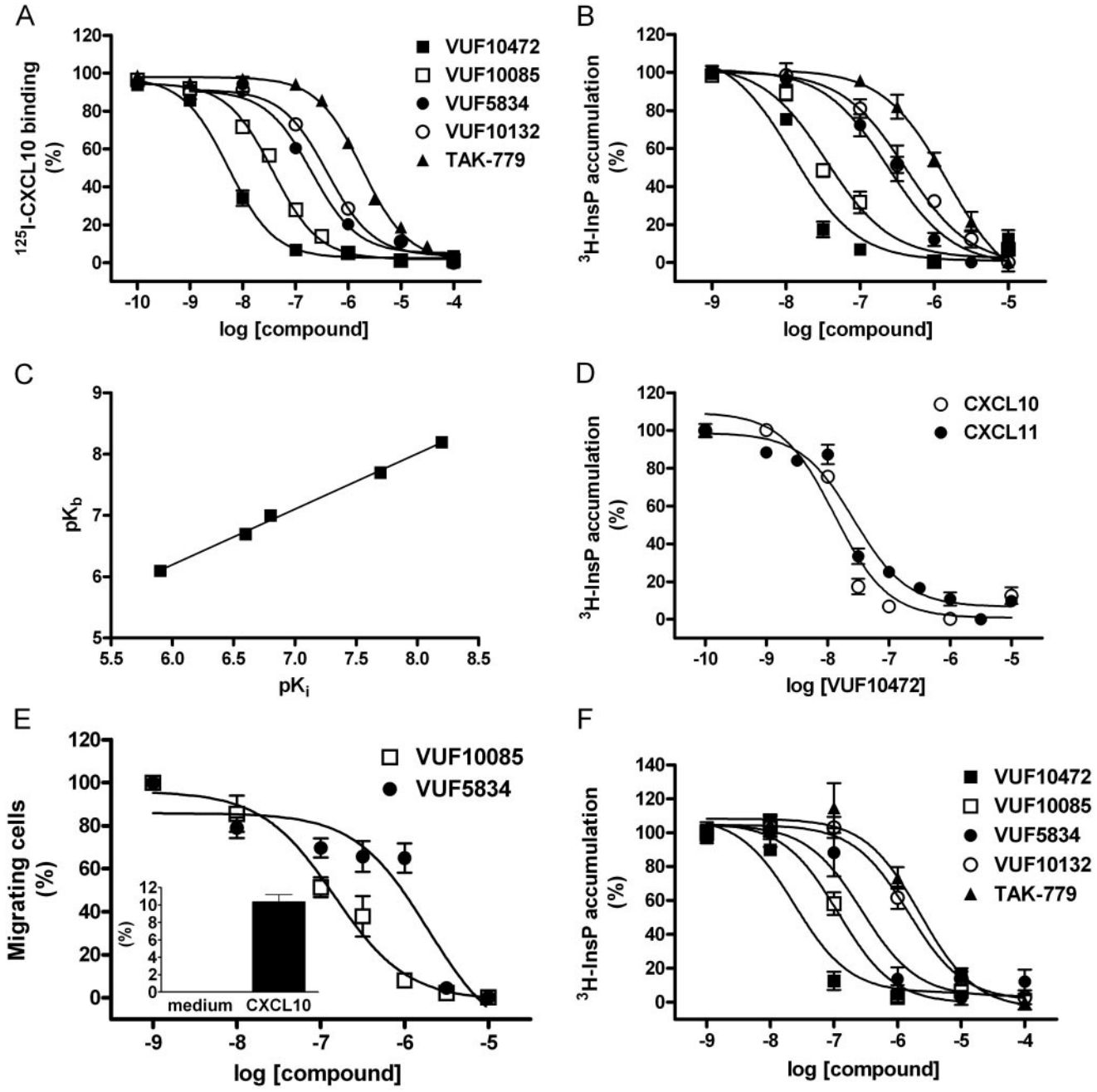

Fig. 5. Characterization of small nonpeptidergic compounds at human CXCR3. A, displacement of ^{125}I-CXCL10. Binding experiments were performed with approximately 50 pM ^{125}I-CXCL10 and increasing concentrations of VUF10472 (■), VUF10085 (□), VUF5834 (●), VUF10132 (○), or TAK-779 (▲) on membranes from HEK293T cells transfected with cDNA encoding human CXCR3. Data are presented as percentage of total binding. pK_i values were 8.4 ± 0.1 (VUF10472; n = 7), 7.7 ± 0.0 (VUF10085; n = 18), 6.8 ± 0.1 (VUF5834; n = 3), 6.6 ± 0.0 (VUF10132; n = 4), and 5.9 ± 0.0 (TAK-779; n = 6). B, inhibition of CXCL10-induced PLC activation. HEK293T cells were transfected with cDNA encoding human CXCR3 and Gα_{qi5}. After 48 h, CXCL10-induced (10–50 nM) [^{3}H]InsP accumulation was determined in the presence of increasing concentrations of VUF10472 (■), VUF10085 (□), VUF5834 (●), VUF10132 (○), or TAK-779 (▲). pK_b values were 8.2 ± 0.1 (VUF10472; n = 5), 7.7 ± 0.1 (VUF10085; n = 9), 7.0 ± 0.1 (VUF5834; n = 5), 6.7 ± 0.1 (VUF10132; n = 5), and 6.1 ± 0.1 (TAK-779; n = 4). C, relationship between pK_i and pK_b of small-molecule compounds. pK_b values obtained using CXCL10 were plotted against pK_i values obtained against ^{125}I-CXCL10 (r^2 = 0.997). D, inhibition of CXCL11-induced PLC activation by VUF10472. HEK293T cells were transfected with cDNA encoding human CXCR3 and Gα_{qi5}. After 48 h, CXCL11-induced (5 nM) [^{3}H]InsP accumulation was determined in the presence of increasing concentrations of VUF10472 (■). The pK_b value of VUF10472 was 7.9 ± 0.0 (n = 3). For comparison, inhibition of CXCL10-induced (50 nM) PLC activation by VUF10472 is shown as well (□). Data are represented as percentage of stimulation in the absence of antagonist. pK_b values were calculated using the Cheng-Prusoff equation (Cheng and Prusoff, 1973). E, inhibition of CXCL10-induced chemotaxis. L1.2 cells were transfected with cDNA encoding human CXCR3. After 24 h, inhibition of CXCL10-induced (10 nM) chemotaxis was determined. pIC_{50} values were 6.8 ± 0.2 (VUF10085; n = 2) and 5.8 ± 0.1 (VUF5834; n = 3). Data are presented as percentage of migrated cells in the absence of antagonist. Inset, CXCL10-induced chemotaxis of L1.2 cells. Data are presented as percentage of total L1.2 cells that migrated to 10 nM CXCL10 in the absence of antagonist (n = 3). F, inhibition of mouse CXCL10-induced PLC activation through mouse CXCR3. HEK293T cells were transfected with cDNA encoding mouse CXCR3 and Gα_{qi5}. After 48 h, mouse CXCL10-induced (20 nM) [^{3}H]InsP accumulation was determined in the presence of increasing concentrations of VUF10472 (■), VUF10085 (□), VUF5834 (●), VUF10132 (○), or TAK-779 (▲). pK_b values were 8.4 ± 0.1 (VUF10472; n = 4), 7.7 ± 0.1 (VUF10085; n = 4), 7.4 ± 0.2 (VUF5834; n = 3), 6.6 ± 0.1 (VUF10132; n = 4), and 6.4 ± 0.1 (TAK-779; n = 4).

TABLE 2

Properties of small nonpeptidergic compounds at CXCR3

pK_i values ± S.E.M. were generated in heterologous radioligand binding experiments using human ^{125}I-CXCL10. pK_b values were obtained at human CXCR3 with human CXCL10 and at mouse CXCR3 with mouse CXCL10 in the PLC activation assay, and pIC_{50} values were generated using human CXCR3 N3.35A in the PLC activation assay.

	pK_i										pK_b				pIC_{50}	
	Human	*n*	N3.35A	*n*	Rhesus	*n*	Rat	*n*	Mouse	*n*	hCXCR3 hCXCL10	*n*	mCXCR3 mCXCL10	*n*	hCXCR3 N3.35A	*n*
VUF10472	8.4 ± 0.1	7	7.9 ± 0.2	3	8.4 ± 0.1	3	7.8 ± 0.0	3	7.9 ± 0.1	3	8.2 ± 0.1	5	8.4 ± 0.1	4	8.1 ± 0.1	3
VUF10085	7.7 ± 0.0	18	7.3 ± 0.1	3	7.5 ± 0.0	3	6.9 ± 0.1	10	7.0 ± 0.1	3	7.7 ± 0.1	9	7.7 ± 0.1	4	8.0 ± 0.1	3
VUF5834	6.8 ± 0.1	3	6.4 ± 0.0	3	6.8 ± 0.0	3	6.2 ± 0.1	6	6.2 ± 0.1	3	7.0 ± 0.1	5	7.4 ± 0.2	3	7.3 ± 0.0	3
VUF10132	6.6 ± 0.0	4	5.9 ± 0.1	3	6.6 ± 0.1	3	6.0 ± 0.1	6	6.0 ± 0.1	3	6.7 ± 0.1	5	6.6 ± 0.1	4	6.6 ± 0.1	3
TAK-779	5.9 ± 0.0	6	5.9 ± 0.0	3	5.9 ± 0.1	3	5.8 ± 0.0	6	5.9 ± 0.0	3	6.1 ± 0.1	4	6.4 ± 0.1	4	5.9 ± 0.1	3

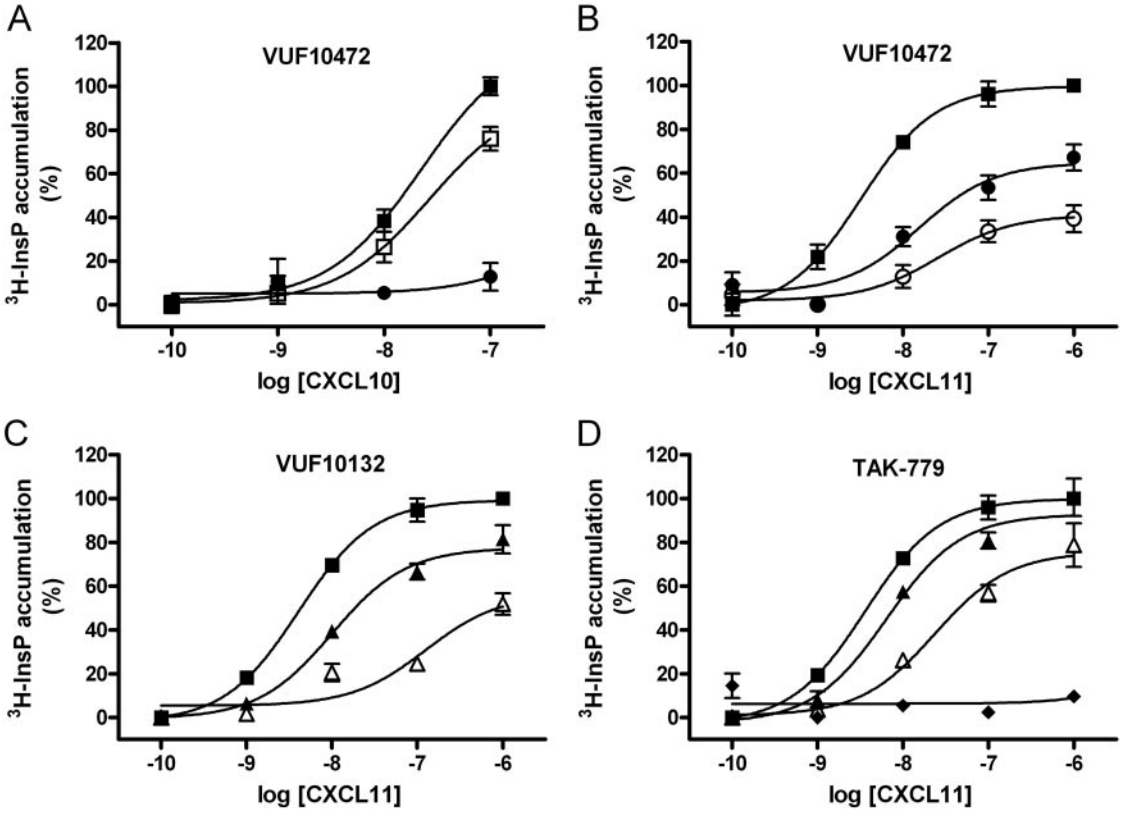

Fig. 6. Noncompetitive behavior of nonpeptidergic compounds at human CXCR3. A, Schild analysis of VUF10472 using CXCL10 as agonist. HEK293T cells were transfected with cDNA encoding human CXCR3 and Gα_{qi5}. After 48 h, CXCL10-induced [^{3}H]InsP accumulation was determined in the absence (■) or in the presence of 10 nM (□) or 30 nM (●) VUF10472 (n = 2–3). B to D, Schild analysis using CXCL11 as agonist. HEK293T cells were transfected with cDNA encoding human CXCR3 and Gα_{qi5}. After 48 h, CXCL11-induced [^{3}H]InsP accumulation was determined in the absence (■) or in the presence of 30 nM (●), 100 nM (○), 1 μM (▲), 10 μM (△), or 100 μM (♦) VUF10472 (B; n = 6), VUF10132 (C; n = 6), or TAK-779 (D; n = 7). Data are presented as percentage of chemokine-induced (1 μM) stimulation in the absence of small-molecule compound.

only CXCL11. VUF10132 (Fig. 6C) and TAK-779 (Fig. 6D) both clearly showed noncompetitive antagonistic behavior similar to that of VUF10472.

Specificity of the Nonpeptidergic CXCR3 Antagonists. The CXCR3 antagonists were tested against a small panel of chemokine and histamine receptors to determine their specificity. HEK293T cells expressing the different GPCRs were incubated with their respective agonists in the presence or absence of CXCR3 antagonists, and activation of PLC was determined. The percentage inhibition of agonist-induced PLC activation by the CXCR3 antagonists is shown in Table 3. As expected, the CXCR3 antagonists (10 μM) showed 50 to 100% inhibition of CXCL11-induced (100 nM) PLC activation through CXCR3, and the CCR5/CCR2/CXCR3 antagonist TAK-779 inhibited CCL2-induced activation of CCR2 with 95%. Unexpectedly, VUF10132 inhibited CCL5-induced CCR1 activation with 61%, compared with 71% inhibition of CXCR3-mediated response. The other CXCR3 antagonists did not significantly inhibit the tested chemokine or histamine receptors (Table 3). In addition, the compounds were tested in radioligand binding studies on membranes expressing CXCR2, CXCR4, or the histamine H_1 receptor. At the tested concentration (10 μM), the CXCR3 antagonists typically inhibit ^{125}I-CXCL10 binding to CXCR3 with 80 to 100% (Fig. 5A). Besides TAK-779, which inhibited binding of [^{3}H]mepyramine to the histamine H_1 receptor with only 41% at 10 μM, no significant inhibition of radioligand binding to CXCR2, CXCR4, or the H_1 receptor by the other CXCR3 antagonists was observed.

Nonpeptidergic Antagonists Are Inverse Agonists at a Constitutively Active Mutant of CXCR3. Inverse agonism has recently been shown to be an important molecular mechanism of action of small-molecule antagonists at a va-

TABLE 3

Selectivity of CXCR3 antagonists

HEK293T cells coexpressing indicated human GPCRs and $G\alpha_{qi5}$ were stimulated with indicated chemokines (100 nM) or histamine (10 μM) in the presence of CXCR3 antagonists (10 μM). The percentage of inhibition of agonist-induced PLC activation is shown. Experiments were performed in duplicate and repeated two (CXCR2) or three times. Radioligand binding studies were performed on membranes of HEK293T (CXCR4) or COS-7 cells (CXCR2 and histamine H_1 receptor). The percentage of inhibition of specific radioligand binding by the CXCR3 antagonists (10 μM) is shown. Experiments were performed in triplicate and repeated two (CXCR2) or three times.

	Inhibition of Agonist-Induced PLC Activation								Inhibition of Specific Binding		
	CXCR3 CXCL11	CXCR1 CXCL8	CXCR2 CXCL1	CXCR4 CXCL12	CCR1 CCL5	CCR2 CCL2	H_1R Histamine	H_3R Histamine	CXCR2 ^{125}I-CXCL8	CXCR4 ^{125}I-CXCL12	H_1R [^{3}H]Mepyramine
	%										
VUF10472	103 ± 8	−19 ± 16	8 ± 1	−7 ± 5	−6 ± 7	11 ± 3	−12 ± 24	−14 ± 2	6 ± 15	17 ± 11	30 ± 13
VUF10085	100 ± 13	−7 ± 17	6 ± 2	1 ± 8	−3 ± 2	10 ± 4	−37 ± 11	−33 ± 14	−15 ± 3	18 ± 7	20 ± 10
VUF5834	67 ± 9	−7 ± 29	13 ± 3	−19 ± 5	−3 ± 13	−1 ± 4	11 ± 17	−35 ± 12	−13 ± 7	0 ± 7	28 ± 11
VUF10132	71 ± 6	−2 ± 10	−33 ± 5	24 ± 2	61 ± 4	−1 ± 11	0 ± 2	−3 ± 8	−21 ± 14	4 ± 12	30 ± 6
TAK-779	53 ± 4	−8 ± 25	−8 ± 4	−2 ± 16	−12 ± 4	95 ± 6	−10 ± 26	−3 ± 15	−12 ± 6	−9 ± 32	41 ± 7

riety of GPCR family members (Parra and Bond, 2007). Human chemokine receptors generally do not show high levels of constitutive activity. However, constitutively active chemokine receptor mutants have been described that signal in the absence of ligands. Examples are CXCR2 D3.49V (Burger et al., 1999), mutation of N3.35 of CXCR4 (Zhang et al., 2002), and mutation of T2.56 in CCR2 and CCR5 (Arias et al., 2003). To determine whether the studied CXCR3 antagonists act as neutral antagonists or inverse agonists at CXCR3, analogous CAMs of CXCR3 were constructed (Fig. 3). Upon expression of the CXCR3 mutants N3.35A, N3.35S, and T2.56P, significant constitutive activity was shown, whereas no constitutive activity was found for the CXCR3 D3.49V mutant (data not shown). In view of the signal-to-noise ratio, we choose CXCR3 N3.35A for further characterization. Upon transfection of HEK293T cells with increasing amounts of cDNA encoding CXCR3 WT or CXCR3 N3.35A, an increase in receptor expression was detected in ELISA experiments (Fig. 7A). When similar amounts of cDNA were transfected, CXCR3 WT was expressed at higher levels than CXCR3 N3.35A (Fig. 7A). As expected, CXCR3 WT did not activate PLC in the absence of ligands (Fig. 7B). Even though CXCR3

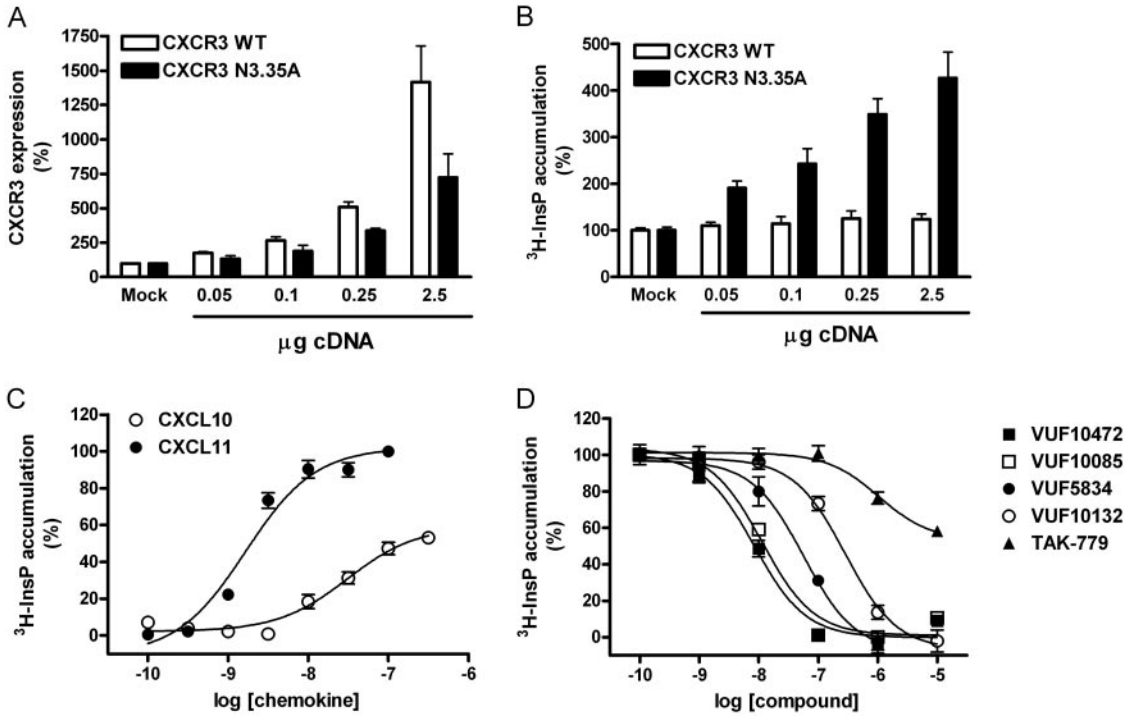

Fig. 7. Characterization of the constitutively active mutant CXCR3 N3.35A. A, expression of CXCR3 WT and CXCR3 N3.35A. HEK293T cells were transfected with cDNA encoding $G\alpha_{qi5}$ and increasing amounts of cDNA encoding human CXCR3 WT or CXCR3 N3.35A. Mock cells were transfected with cDNA encoding $G\alpha_{qi5}$ and pcDEF3 empty vector. After 48 h, CXCR3 expression was determined in an ELISA assay. Data are presented as percentage signal obtained in mock-transfected cells (n = 2–3). B, constitutive activity of CXCR3 N3.35A. HEK293T cells were transfected with cDNA encoding $G\alpha_{qi5}$ and increasing amounts of cDNA encoding human CXCR3 WT or CXCR3 N3.35A. Mock cells were transfected with cDNA encoding $G\alpha_{qi5}$ and pcDEF3 empty vector. After 48 h, [^{3}H]InsP accumulation was determined in the absence of chemokines. Data are presented as percentage of [^{3}H]InsP in mock-transfected cells (n = 3). C, chemokine-induced PLC activation by CXCR3 N3.35A. HEK293T cells were transfected with cDNA encoding CXCR3 N3.35A and $G\alpha_{qi5}$. After 48 h, [^{3}H]InsP accumulation was determined in the presence of increasing concentrations CXCL10 or CXCL11. pEC_{50} values for CXCL10 and CXCL11 were 7.5 ± 0.0 (n = 2) and 8.7 ± 0.1 (n = 4), respectively. Data are presented as percentage of the maximal response obtained with CXCL11 (100 nM). D, inverse agonism at CXCR3 N3.35A. HEK293T cells were transfected with cDNA encoding CXCR3 N3.35A and $G\alpha_{qi5}$. After 48 h, [^{3}H]InsP accumulation was determined in the presence of increasing concentrations VUF10472 (■), VUF10085 (□), VUF5834 (●), VUF10132 (○), or TAK-779 (▲). pIC_{50} values (n = 3) were 8.1 ± 0.1 (VUF10472), 8.0 ± 0.1 (VUF10085), 7.3 ± 0.0 (VUF5834), 6.6 ± 0.1 (VUF10132), and 5.9 ± 0.1 (TAK-779). Data are presented as percentage of CXCR3 N3.35A-mediated constitutive [^{3}H]InsP accumulation.

N3.35A was expressed at lower levels than CXCR3 WT, CXCR3 N3.35A showed a marked increase of PLC activation upon transfection of increasing amounts of cDNA (Fig. 7B).

The affinities of CXCL10 (pK_d of 10.2 ± 0.2) and CXCL11 (pK_d of 11.3 ± 0.3) for CXCR3 N3.35A were slightly higher than for CXCR3 WT (Table 1). CXCL10 and CXCL11 activated CXCR3 N3.35A over basal levels in a similar manner as CXCR3 WT, with pEC_{50} values of 7.5 ± 0.0 (n = 2) and 8.7 ± 0.1 (n = 4), respectively (Fig. 7C; Table 1). Subsequently, the affinity of the small-molecule antagonists at CXCR3 N3.35A was determined using ^{125}I-CXCL10. The affinity of all compounds, except TAK-779, was slightly reduced for CXCR3 N3.35A compared with CXCR3 WT (Table 2). Finally, the effect of the small-molecule antagonists on the constitutive activation of PLC was investigated. VUF10472, VUF10085, VUF5834, and VUF10132 all acted as full inverse agonists, with IC_{50} values ranging between 8 nM for VUF10472 and 251 nM for VUF10132 (Fig. 7D; Table 2). In contrast, TAK-779 acted as a partial inverse agonist, with an intrinsic activity of −0.42 ± 0.0 and an IC_{50} of 1.3 μM (n = 3) (Fig. 7D; Table 2).

Discussion

CXCR3 has attracted considerable attention as a new drug target due to its involvement in a variety of serious disorders, including cancer (Walser et al., 2006), atherosclerosis (Mach et al., 1999), inflammatory disorders such as rheumatoid arthritis (Qin et al., 1998), skin diseases (Flier et al., 2001), and transplant rejection (Hancock et al., 2000). After the recognition of CXCR3 as a potential attractive drug target, several small-molecule CXCR3 antagonists have recently been identified (Gao et al., 2003; Heise et al., 2005; Storelli et al., 2005; Cole et al., 2006; Allen et al., 2007; Johnson et al., 2007; Storelli et al., 2007). In this study, we selected five nonpeptidergic antagonists from four different structural classes, and we studied their mechanism of action at the human CXCR3. In addition, the interaction of these antagonists with human, rhesus macaque, rat, and mouse CXCR3 was investigated.

All tested nonpeptidergic antagonists inhibited CXCL10-induced activation of PLC, with pK_b values that correlated very well with their affinity, with a rank order VUF10472 > VUF10085 > VUF5834 > VUF10132 > TAK-779 (Table 2). Subsequently, the mechanism of action of the antagonists was explored using Schild analysis. The dose-response curves for CXCL10 and CXCL11 did not reach the maximal response in the presence of VUF10472 (Fig. 6), as has been shown previously by others for human and mouse CXCR3 (Heise et al., 2005; Jopling et al., 2007). Antagonists from other structural classes also decreased the maximum response of CXCL11, in a manner that follows the rank order of their affinities. This indicates that all tested nonpeptidergic antagonists behave as noncompetitive antagonists for the PLC activation by the endogenous agonists of CXCR3.

Antagonists of GPCRs can be classified as neutral antagonists or (partial) inverse agonists (Kenakin, 1996; Parra and Bond, 2007). Although both antagonist classes are able to block an agonist-induced response by occupying the receptor, there is an ongoing debate about the exact clinical benefits or disadvantages of each class (Parra and Bond, 2007). Treatment with inverse agonists may be beneficial when a constitutively active receptor underlies the pathogenesis. To date, there are no reports about constitutive activity of CXCR3, and there are only few examples of constitutive activity of chemokine receptors. Constitutive activity is a function of the relative stoichiometry of receptors and G proteins (Kenakin, 1996), and chemokine receptors, including CXCR3, are often up-regulated under inflammatory conditions (Rabin et al., 1999; Murphy et al., 2000). Hence, under pathophysiological conditions constitutive activity of chemokine receptors might become apparent; therefore, the use of inverse agonists beneficial. To study the relative efficacy of the nonpeptidergic antagonists, we generated mutants of CXCR3, i.e., CXCR3 N3.35A, N3.35S, D3.39V, and T2.56P, based on CAMs of chemokine receptors reported in literature (Burger et al., 1999; Zhang et al., 2002; Arias et al., 2003). All generated mutants, except for CXCR3 D3.49V with a mutation in the conserved DRY motif at the cytoplasmatic end of TM3, displayed basal signaling. Mutation of the DRY motif of CXCR2 to VRY confers constitutive activity to CXCR2 (Burger et al., 1999), whereas the same mutation for CXCR1 (Burger et al., 1999) or CCR5 (Lagane et al., 2005) did not result in constitutive activity. In contrast, mutation of the VRY motif to DRY in the highly constitutively active chemokine receptor ORF74 encoded by Kaposi's sarcoma-associated herpesvirus did not diminish its constitutive activity but even increased it (Ho et al., 2001). Therefore, mutation of D3.49 to Val does not seem to be a universal switch for constitutive activity in chemokine receptors. In the same way, mutation of T2.56 in the conserved TXP motif resulted in a CAM for CXCR3 (this study), CCR5, and CCR2, but not for CCR1, CCR3, CCR4, CXCR2, and CXCR4 (Arias et al., 2003). Mutation of N3.35 in the N(L/F)Y motif in TM3 of CXC chemokine receptors resulted in CAMs for both CXCR3 (this study) and CXCR4 (Zhang et al., 2002). The nonpeptidergic compounds acted as full inverse agonists at CXCR3 N3.35A, except for TAK-779, which only partially inhibited constitutive signaling at the highest concentration used (Fig. 7D). Because VUF10132 and TAK-779 have similar affinities for CXCR3 N3.35A (Table 2), it seems that TAK-779 lacks certain structural features needed for full inverse agonism at CXCR3. It is interesting to note that TAK-779 acts as a full inverse agonist at CCR5 (Lagane et al., 2005). As expected for a receptor in the active state (Kenakin, 1996), the affinities of the agonists CXCL10 and CXCL11 for CXCR3 N3.35A were increased compared with CXCR3 WT (Table 1). The full inverse agonists VUF10472, VUF10085, VUF5834, and VUF10132, which are predicted to have a higher affinity for an inactive receptor conformation (Kenakin, 1996), all showed reduced affinity for CXCR3 N3.35A compared with CXCR3 WT (Table 2). In contrast, the affinity of the weak partial inverse agonist TAK-779 did not change, indicating a different mode of interaction with CXCR3 compared with the other structural classes of compounds.

If antagonists are to be tested in animal models, detailed information on the interaction of the compound with the receptor of that specific species is required, because species differences may occur. We therefore tested the nonpeptidergic antagonists on rhesus macaque CXCR3, which was cloned in this study, as well as on rat and mouse CXCR3. Human and rhesus macaque show 99% amino acid identity (Fig. 3). Consistent with this high homology, no differences in affinity or potency of CXCL10 and CXCL11, or in the affinity of the nonpeptidergic

antagonists for the two receptors were found. Likewise, the protein sequences of rat and mouse CXCR3 are 96% identical, and no significant differences in affinity of the endogenous agonists or the nonpeptidergic compounds are observed between the CXCR3 of these rodent species. However, lower sequence identity is found when human and rhesus macaque CXCR3s are compared with rat and mouse CXCR3. Approximately 85% identity exists between the primate (human and rhesus macaque) and rodent (rat and mouse) species (Fig. 3). Nevertheless, the affinities of CXCL10 and CXCL11 found for rodent CXCR3 were comparable with the affinities found for primate CXCR3 (Table 1). Although the affinities of CXCL10 and CXCL11 were comparable, the affinities of VUF10472, VUF10084, VUF5834, and VUF101032 were only approximately 4-fold lower for rodent CXCR3 than for primate CXCR3 (Table 2). In addition, their pK_b values against hCXCL10/hCXCR3 and mCXCL10/mCXCR3 are comparable (Table 2; Fig. 5, B and F), indicating the usefulness of these compounds in mouse models. In contrast, the affinity of TAK-779 was equal for CXCR3 of all tested species, again indicating that TAK-779 interacts with CXCR3 in another manner than the other small-molecule antagonists. TAK-779, developed as a CCR5 antagonist, has been thoroughly investigated because of its potential use as a human immunodeficiency virus-entry inhibitor. TAK-779 shows high affinity for human CCR5 and to a lesser extent for human CCR2b (Baba et al., 1999). Furthermore, TAK-779 was reported to bind mouse CCR5, as well as mouse CXCR3 (Gao et al., 2003). It is remarkable that TAK-779 shows a more than 100-fold higher affinity for human CCR5 than for mouse CCR5 (Baba et al., 1999; Gao et al., 2003). This species selectivity of TAK-779 for CCR5 is not observed for human and mouse CXCR3, which both bind TAK-779 with affinities around 1 μM (Table 2). It seems that TAK-779 has nanomolar affinity for human CCR5 and micromolar affinity for human CXCR3, whereas it has only micromolar affinity for mouse CCR5 and mouse CXCR3. This should be kept in mind when analyzing and extrapolating data from rodent models, because at a certain effective concentration of TAK-779 different receptors will be occupied in humans and mice. Although in mice the observed effects would probably be mediated by a combination of blockage of CCR5 and CXCR3, in humans the effects of TAK-779 would be mostly through inhibition of CCR5 with low nanomolar affinity. The nonpeptidergic CXCR3 antagonists investigated here only showed a 3- to 4-fold species selectivity for CXCR3 of primates versus rodents in radioligand binding studies, whereas no species difference was observed in functional studies. When testing for selectivity against a panel of GPCRs, VUF10132 inhibited CCR1-mediated signaling, and it should therefore be optimized with respect to its affinity and specificity for CXCR3. In contrast, we observed that VUF10472, VUF10085, and VUF5834 are selective for CXCR3. In line with our findings, VUF10472/NBI-74330 has been reported previously not to affect chemotactic responses by human H9 T-cell lymphoma cells in response to CXCL12 and CCL19 and not to interfere with calcium mobilization induced by lysophosphatidic acid or radioligand binding to several GPCRs (Heise et al., 2005).

In summary, we characterized three classes of small nonpeptidergic and noncompetitive CXCR3 antagonists at CXCR3 of four different species, with VUF10472 being the most potent compound at human, rhesus, rat, and mouse CXCR3. The observed selectivity profile and relatively small difference in affinity observed between human and rodent CXCR3 imply that VUF10472/NBI-74330, VUF10085/AMG-487, and VUF5834 are useful in rodent models of CXCR3-mediated pathogenesis. Interestingly, it was found that the nonpeptidergic antagonists act as inverse agonists at a constitutively active CXCR3 mutant.

Acknowledgments

We thank Kamonchanok Sansuk and Anne O. Watts for help with some of the experiments.

References

Allen DR, Bolt A, Chapman GA, Knight RL, Meissner JW, Owen DA, and Watson RJ (2007) Identification and structure-activity relationships of 1-aryl-3-piperidin-4-yl-urea derivatives as CXCR3 receptor antagonists. *Bioorg Med Chem Lett* **17:**697–701.

Arias DA, Navenot JM, Zhang WB, Broach J, and Peiper SC (2003) Constitutive activation of CCR5 and CCR2 induced by conformational changes in the conserved TXP motif in transmembrane helix 2. *J Biol Chem* **278:**36513–36521.

Axten JM, Foley JJ, Kingsbury WD, and Sarau HM (2003) inventors; SmithKline Beechham Corporation, assignee. Imidazolium CXCR3 inhibitors. World patent WO031101970. 2003 Dec 11.

Baba M, Nishimura O, Kanzaki N, Okamoto M, Sawada H, Iizawa Y, Shiraishi M, Aramaki Y, Okonogi K, Ogawa Y, et al. (1999) A small-molecule, nonpeptide CCR5 antagonist with highly potent and selective anti-HIV-1 activity. *Proc Natl Acad Sci U S A* **96:**5698–5703.

Ballesteros JA and Weinstein H (1995) Integrated methods for the construction of three dimensional models and computational probing of structure-function relations in G-protein coupled receptors. *Methods Neurosci* **25:**366–428.

Burger M, Burger JA, Hoch RC, Oades Z, Takamori H, and Schraufstatter IU (1999) Point mutation causing constitutive signaling of CXCR2 leads to transforming activity similar to Kaposi's sarcoma herpesvirus-G protein-coupled receptor. *J Immunol* **163:**2017–2022.

Cheng Y and Prusoff WH (1973) Relationship between the inhibition constant (K1) and the concentration of inhibitor which causes 50 per cent inhibition (I50) of an enzymatic reaction. *Biochem Pharmacol* **22:**3099–3108.

Cole AG, Stroke IL, Brescia MR, Simhadri S, Zhang JJ, Hussain Z, Snider M, Haskell C, Ribeiro S, Appell KC, et al. (2006) Identification and initial evaluation of 4-N-aryl-[1,4]diazepane ureas as potent CXCR3 antagonists. *Bioorg Med Chem Lett* **16:**200–203.

Cole KE, Strick CA, Paradis TJ, Ogborne KT, Loetscher M, Gladue RP, Lin W, Boyd JG, Moser B, Wood DE, et al. (1998) Interferon-inducible T cell alpha chemoattractant (I-TAC): a novel non-ELR CXC chemokine with potent activity on activated T cells through selective high affinity binding to CXCR3. *J Exp Med* **187:**2009–2021.

Coward P, Chan SD, Wada HG, Humphries GM, and Conklin BR (1999) Chimeric G proteins allow a high-throughput signaling assay of Gi-coupled receptors. *Anal Biochem* **270:**242–248.

Flier J, Boorsma DM, van Beek PJ, Nieboer C, Stoof TJ, Willemze R, and Tensen CP (2001) Differential expression of CXCR3 targeting chemokines CXCL10, CXCL9, and CXCL11 in different types of skin inflammation. *J Pathol* **194:**398–405.

Gao P, Zhou XY, Yashiro-Ohtani Y, Yang YF, Sugimoto N, Ono S, Nakanishi T, Obika S, Imanishi T, Egawa T, et al. (2003) The unique target specificity of a nonpeptide chemokine receptor antagonist: selective blockade of two Th1 chemokine receptors CCR5 and CXCR3. *J Leukoc Biol* **73:**273–280.

Hancock WW, Lu B, Gao W, Csizmadia V, Faia K, King JA, Smiley ST, Ling M, Gerard NP, and Gerard C (2000) Requirement of the chemokine receptor CXCR3 for acute allograft rejection. *J Exp Med* **192:**1515–1520.

Heise CE, Pahuja A, Hudson SC, Mistry MS, Putnam AL, Gross MM, Gottlieb PA, Wade WS, Kiankarimi M, Schwarz D, et al. (2005) Pharmacological characterization of CXC chemokine receptor 3 ligands and a small molecule antagonist. *J Pharmacol Exp Ther* **313:**1263–1271.

Hensbergen PJ, Wijnands PG, Schreurs MW, Scheper RJ, Willemze R, and Tensen CP (2005) The CXCR3 targeting chemokine CXCL11 has potent antitumor activity in vivo involving attraction of $CD8^+$ T lymphocytes but not inhibition of angiogenesis. *J Immunother* **28:**343–351.

Ho HH, Ganeshalingam N, Rosenhouse-Dantsker A, Osman R, and Gershengorn MC (2001) Charged residues at the intracellular boundary of transmembrane helices 2 and 3 independently affect constitutive activity of Kaposi's sarcoma-associated herpesvirus G protein-coupled receptor. *J Biol Chem* **276:**1376–1382.

Johnson M, Li AR, Liu J, Fu Z, Zhu L, Miao S, Wang X, Xu Q, Huang A, Marcus A, et al. (2007) Discovery and optimization of a series of quinazolinone-derived antagonists of CXCR3. *Bioorg Med Chem Lett* **17:**3339–3343.

Jopling LA, Watt GF, Fisher S, Birch H, Coggon S, and Christie MI (2007) Analysis of the pharmacokinetic/pharmacodynamic relationship of a small molecule CXCR3 antagonist, NBI-74330, using a murine CXCR3 internalization assay. *Br J Pharmacol* **152:**1260–1271.

Kenakin T (1996) The classification of seven transmembrane receptors in recombinant expression systems. *Pharmacol Rev* **48:**413–463.

Lagane B, Ballet S, Planchenault T, Balabanian K, Le Poul E, Blanpain C, Percherancier Y, Staropoli I, Vassart G, Oppermann M, et al. (2005) Mutation of the DRY motif reveals different structural requirements for the CC chemokine receptor 5-mediated signaling and receptor endocytosis. *Mol Pharmacol* **67:**1966–1976.

Loetscher M, Gerber B, Loetscher P, Jones SA, Piali L, Clark-Lewis I, Baggiolini M,

and Moser B (1996) Chemokine receptor specific for IP10 and mig: structure, function, and expression in activated T-lymphocytes. *J Exp Med* **184:**963–969.
Lu B, Humbles A, Bota D, Gerard C, Moser B, Soler D, Luster AD, and Gerard NP (1999) Structure and function of the murine chemokine receptor CXCR3. *Eur J Immunol* **29:**3804–3812.
Luster AD and Leder P (1993) IP-10, a -C-X-C- chemokine, elicits a potent thymus-dependent antitumor response in vivo. *J Exp Med* **178:**1057–1065.
Mach F, Sauty A, Iarossi AS, Sukhova GK, Neote K, Libby P, and Luster AD (1999) Differential expression of three T lymphocyte-activating CXC chemokines by human atheroma-associated cells. *J Clin Invest* **104:**1041–1050.
Murphy PM, Baggiolini M, Charo IF, Hebert CA, Horuk R, Matsushima K, Miller LH, Oppenheim JJ, and Power CA (2000) International union of pharmacology. XXII. Nomenclature for chemokine receptors. *Pharmacol Rev* **52:**145–176.
Pan J, Burdick MD, Belperio JA, Xue YY, Gerard C, Sharma S, Dubinett SM, and Strieter RM (2006) CXCR3/CXCR3 ligand biological axis impairs RENCA tumor growth by a mechanism of immunoangiostasis. *J Immunol* **176:**1456–1464.
Parra S and Bond RA (2007) Inverse agonism: from curiosity to accepted dogma, but is it clinically relevant? *Curr Opin Pharmacol* **7:**146–150.
Qin S, Rottman JB, Myers P, Kassam N, Weinblatt M, Loetscher M, Koch AE, Moser B, and Mackay CR (1998) The chemokine receptors CXCR3 and CCR5 mark subsets of T cells associated with certain inflammatory reactions. *J Clin Invest* **101:**746–754.
Rabin RL, Park MK, Liao F, Swofford R, Stephany D, and Farber JM (1999) Chemokine receptor responses on T cells are achieved through regulation of both receptor expression and signaling. *J Immunol* **162:**3840–3850.
Salomon I, Netzer N, Wildbaum G, Schif-Zuck S, Maor G, and Karin N (2002) Targeting the function of IFN-gamma-inducible protein 10 suppresses ongoing adjuvant arthritis. *J Immunol* **169:**2685–2693.
Smit MJ, Verdijk P, van der Raaij-Helmer EM, Navis M, Hensbergen PJ, Leurs R, and Tensen CP (2003) CXCR3-mediated chemotaxis of human T cells is regulated by a Gi- and phospholipase C-dependent pathway and not via activation of MEK/p44/p42 MAPK nor Akt/PI-3 kinase. *Blood* **102:**1959–1965.
Sørensen TL, Tani M, Jensen J, Pierce V, Lucchinetti C, Folcik VA, Qin S, Rottman J, Sellebjerg F, Strieter RM, et al. (1999) Expression of specific chemokines and chemokine receptors in the central nervous system of multiple sclerosis patients. *J Clin Invest* **103:**807–815.
Storelli S, Verdijk P, Verzijl D, Timmerman H, van de Stolpe AC, Tensen CP, Smit MJ, De Esch IJ, and Leurs R (2005) Synthesis and structure-activity relationship of 3-phenyl-3H-quinazolin-4-one derivatives as CXCR3 chemokine receptor antagonists. *Bioorg Med Chem Lett* **15:**2910–2913.
Storelli S, Verzijl D, Al-Badie J, Elders N, Bosch L, Timmerman H, Smit MJ, De Esch IJ, and Leurs R (2007) Synthesis and structure-activity relationships of 3H-quinazolin-4-ones and 3H-pyrido[2,3-d]pyrimidin-4-ones as CXCR3 receptor antagonists. *Arch Pharm (Weinheim)* **340:**281–291.
Streblow DN, Kreklywich C, Yin Q, De La Melena VT, Corless CL, Smith PA, Brakebill C, Cook JW, Vink C, Bruggeman CA, et al. (2003) Cytomegalovirus-mediated upregulation of chemokine expression correlates with the acceleration of chronic rejection in rat heart transplants. *J Virol* **77:**2182–2194.
Tamaru M, Tominaga Y, Yatsunami K, and Narumi S (1998) Cloning of the murine interferon-inducible protein 10 (IP-10) and its specific expression in lymphoid organs. *Biochem Biophys Res Commun* **251:**41–48.
Walser TC, Rifat S, Ma X, Kundu N, Ward C, Goloubeva O, Johnson MG, Medina JC, Collins TL, and Fulton AM (2006) Antagonism of CXCR3 inhibits lung metastasis in a murine model of metastatic breast cancer. *Cancer Res* **66:**7701–7707.
Wang X, Li X, Schmidt DB, Foley JJ, Barone FC, Ames RS, and Sarau HM (2000) Identification and molecular characterization of rat CXCR3: receptor expression and interferon-inducible protein-10 binding are increased in focal stroke. *Mol Pharmacol* **57:**1190–1198.
Yang YF, Mukai T, Gao P, Yamaguchi N, Ono S, Iwaki H, Obika S, Imanishi T, Tsujimura T, Hamaoka T, et al. (2002) A non-peptide CCR5 antagonist inhibits collagen-induced arthritis by modulating T cell migration without affecting anti-collagen T cell responses. *Eur J Immunol* **32:**2124–2132.
Zhang WB, Navenot JM, Haribabu B, Tamamura H, Hiramatu K, Omagari A, Pei G, Manfredi JP, Fujii N, Broach JR, et al. (2002) A point mutation that confers constitutive activity to CXCR4 reveals that T140 is an inverse agonist and that AMD3100 and ALX40-4C are weak partial agonists. *J Biol Chem* **277:**24515–24521.

Address correspondence to: Dr. Rob Leurs, Leiden/Amsterdam Center of Drug Research, Faculty of Science, Vrije Universiteit Amsterdam, De Boelelaan 1083, 1081 HV Amsterdam, The Netherlands. E-mail: r.leurs@few.vu.nl